Application of Non-Steady-State Kinetics to Resolve the Kinetics of Proton-Transfer Reactions between Methylarene Radical Cations and Pyridine Bases

Vernon D. Parker,* Yixing Zhao, Yun Lu, and Gang Zheng

Contribution from the Department of Chemistry and Biochemistry, Utah State University, Logan, Utah 84322-0300

Received July 28, 1998

Abstract: Apparent deuterium kinetic isotope effects (KIE_{app}) of four different methylarene radical cation−pyridine base reactions in dichloromethane (0.2 M tetrabutylammonium hexafluorophosphate) were observed to increase toward a constant value with increasing extent of reaction. The reactions were studied by derivative cyclic voltammetry (DCV), and rate constants were assigned by comparing the experimental with the theoretical DCV data. The kinetic results rule out a simple second-order proton-transfer reaction and implicate a mechanism in which a complex is first formed that then undergoes proton transfer, followed by separation of the products. That KIE_{app} are extent of reaction-dependent is observed before steady-state is reached. The concurrent analysis of kinetic data for the reactions of both $ArCH_3^{\bullet+}$ and $ArCD_3^{\bullet+}$ with bases under non-steady-state conditions facilitates the resolution of the apparent rate constant [$k_{app} = k_f k_p/(k_b + k_p)$] into the microscopic rate constants (k_f, k_b, and k_p) for the individual steps. The KIE_{app} observed during proton-transfer reactions need not be the real kinetic isotope effects (KIE_{real}). Having access to the microscopic rate constants for the steps in which the proton is transferred allows KIE_{real} to be evaluated and compared with the corresponding KIE_{app}. The present study shows that the KIE_{real} are much greater than the KIE_{app} derived in the usual way from the rate of the overall reaction.

Introduction

The classical work of Brønsted,[1] Eigen,[2] and Bell[3] as well as diverse contributions of a host of other workers[4] over the past 75 years has provided an immense foundation of knowledge on the most-studied class of chemical reactions, proton transfer from acids to bases. A three-step mechanism for proton transfer—(i) the formation of an encounter complex, (ii) proton transfer to form a new complex, and (iii) separation to products—generally accepted from the work of Eigen.[2] In fact, pointed out by Eigen, it is not a simple matter to determine which of the three steps is rate-determining. Resolution of the kinetics of these reactions, with the assignment of rate constants for all steps, has never been accomplished.

Proton-transfer reactions involving C−H bond cleavage most often take place at rates very much lower than expected for the formation of encounter complexes. Reactions that follow the Eigen mechanism under these conditions are expected to behave kinetically as simple second-order reactions, with apparent rate constants (k_{app}) reflecting both the equilibrium constant (K_{eq}) for the formation of the encounter complex and the rate constant for proton transfer (k_p).

We now report kinetic studies of a series of reactions of methylarene radical cations involving C−H bond cleavage that suggest the formation (k_f) of longer-lived complexes that partition between complex dissociation (k_b) and irreversible proton transfer (k_p) as illustrated in eq 1. Unlike the case

$$HA + B \underset{k_b}{\overset{k_f}{\rightleftharpoons}} HA/B \xrightarrow{k_p} A^-/BH^+ \qquad (1)$$

discussed in the previous paragraph, when k_p and k_b are of comparable magnitude, it is feasible to resolve k_{app} into the rate constants for the individual microscopic steps.

Most organic radical cations are exceedingly strong acids and some are superacids.[5−10] This fact suggests that when HA is a radical cation and B is a relatively strong base, such as pyridine, the proton-transfer reaction will be thermodynamically favorable. The kinetics of several radical cation−base reactions have been reported.[11] Many of these reactions are believed[12,13] to pass

(1) Brønsted, J. N.; Petersen, K. *Z. Phys. Chim.* **1924**, *108*, 185.
(2) Eigen, M. *Angew. Chem., Int. Ed. Engl.* **1964**, *3*, 1.
(3) Bell, R. P. *The Proton in Chemistry*; (Chapman & Hall: London, 1973).
(4) A review of much of the early work can be found in ref 3.
(5) Nicholas, A. M.; Arnold, D. R. *Can. J. Chem.* **1982**, *60*, 2165.
(6) Nicholas, A. M.; Boyd, R. J.; Arnold, D. R. *Can. J. Chem.* **1982**, *60*, 3011.
(7) Bordwell, F. G.; Cheng, J.-P. *J. Am. Chem. Soc.* **1989**, *111*, 1792.
(8) Zhang, X.; Bordwell, F. G. *J. Org. Chem.* **1992**, *57*, 4163.
(9) Zhang, X.; Bordwell, F. G.; Bares, J. E.; Cheng, J.-P.; Petrie, B. C. *J. Org. Chem.* **1993**, *58*, 3051.
(10) Cheng, J.-P. Ph.D. Dissertation, Northwestern University: Evanston, IL, 1987.
(11) Schlesener, C. J.; Amatore, C.; Kochi, J. K. *J. Am. Chem. Soc.* **1984**, *106*, 3567; Schlesener, C. J.; Amatore, C.; Kochi, J. K. *J. Am. Chem. Soc.* **1984**, *106*, 7472; Parker, V. D.; Tilset, M. *J. Am. Chem. Soc.* **1986**, *108*, 6371; Tolbert, L. M.; Khanna, R. K. *J. Am. Chem. Soc.* **1987**, *109*, 3477; Dinnocenzo, J. P.; Banach, T. E. *J. Am. Chem. Soc.* **1989**, *111*, 8646; Tolbert, L. M.; Khanna, R. K.; Popp, A. E.; Gelbaum, L.; Bettomly, L. A. *J. Am. Chem. Soc.* **1990**, *112*, 2373; Reitstöen, B.; Parker, V. D. *J. Am. Chem. Soc.* **1990**, *112*, 4968; Baciocchi, E.; Mattioli, M.; Romano, R.; Ruzziconi, R. *J. Org. Chem.* **1991**, *56*, 7154; Xu, W.; Mariano, P. S. *J. Am. Chem. Soc.* **1991**, *113*, 1431; Steadman, J.; Syage, J. A. *J. Am. Chem. Soc.* **1991**, *113*, 6786; Xu, W.; Zhang, X.-M.; Mariano, P. S. *J. Am. Chem. Soc.* **1991**, *113*, 8863; Anne, A.; Hapiot, P.; Moiroux, J.; Neta, P.; Saveant, J.-M. *J. Am. Chem. Soc.* **1992**, *114*, 4694; Baciocchi, E.; Giacco, T. D.; Elisei, F. *J. Am. Chem. Soc.* **1993**, *115*, 12290; Dinnocenzo, J. P.; Karki, S. B.; Jones, J. P. *J. Am. Chem. Soc.* **1993**, *115*, 7111; Xue, J.-Y.; Parker, V. D. *J. Org. Chem.* **1994**, *59*, 6564.

10.1021/ja982682k CCC: $15.00
Published on Web 11/25/1998

Chart 1

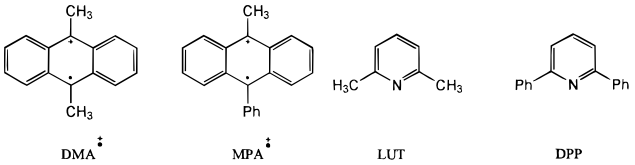

through intermediates, suggested to be π-complexes, within which proton transfer takes place. Previous work provided indirect evidence, including negative apparent activation energies[12] and kinetic isotope effects (KIE),[13] which are readily explained by the complex mechanism.

Results

The structures of the radical cations for 9,10-dimethylanthracene (DMA$^{\bullet+}$) and 9-methyl-10-phenylanthracene (MPA$^{\bullet+}$) and bases (LUT) and 2,6-diphenylpyridine (DPP) studied are shown in Chart 1. The overall reactions, in which the proton-transfer steps are rate determining, are illustrated by general stoichiometric eq 2.

$$2ArCH_3^{\bullet+} + 2B \rightarrow ArCH_2{-}B^+ + BH^+ + ArCH_3 \quad (2)$$

Products of the reactions between both of the radical cations and LUT have previously been characterized.[13,14]

Our kinetic studies were carried out with derivative cyclic voltammetry (DCV), a refinement[15] of the widely used electrochemical transient technique, cyclic voltammetry.[16] DCV has been used extensively in the study of the kinetics of the reactions of radical ions in solution.[12,13,17] The magnitude of the ratio of the derivative peaks ($R'_I = I'_b/I'_f$) is a measure of the rate of reaction of the electrode-generated intermediate, ranging from 1.0 for no reaction to 0 for complete reaction during the time of the experiment. The experimental variable is ν, the voltage sweep rate. The experimental R'_I vs ν^{-1} response curves may be compared with theoretical data obtained by digital simulation[18] to evaluate rate constants of the homogeneous chemical reactions coupled to the charge-transfer reaction of the substrate.

Experimental DCV Data for Radical Cation Proton-Transfer Reactions. DCV data (R'_I ranging from 0.85 to 0.50) were obtained for the reactions of DMA$^{\bullet+}$ (and DMA-$d_6^{\bullet+}$) with LUT in dichloromethane−tetrabutylammonium hexafluorophosphate (Bu_4NPF_6) (0.2 M) at 291 K. The two data sets are shown in Figure 1. The experimental data deviate significantly from the dashed lines, which are the theoretical data obtained by digital simulations for a simple second-order proton-transfer mechanism. Data for the reactions of these radical cations with both LUT and DPP are summarized in Table 1. Values for the apparent deuterium kinetic isotope effects (KIE_{app}) were obtained from $(\nu_H)_{exp}/(\nu_D)_{exp}$ ratios, which are equivalent to $(k_H/k_D)_{app}$ values.[15] Comparable data for the reactions of MPA$^{\bullet+}$ and MPA-$d_3^{\bullet+}$ with LUT and DPP are tabulated in Table 2. Apparent second-order rate constants (k_{app}) for all reactions, calculated from the comparison of experimental DCV data ($R'_I = 0.50$ and 0.55) with those from digital simulation[15] assuming a simple second-order proton-transfer mechanism, are gathered in Table 3.

The most interesting feature of the data for all four reactions is that KIE_{app} vary with R'_I and approach constant values at about $R'_I = 0.50$ (at this R'_I, the reverse peak on the cyclic voltammogram is still visible). The expected result for a single-step second-order proton-transfer reaction is that KIE_{app} will be a constant, independent of the extent of reaction (proportional

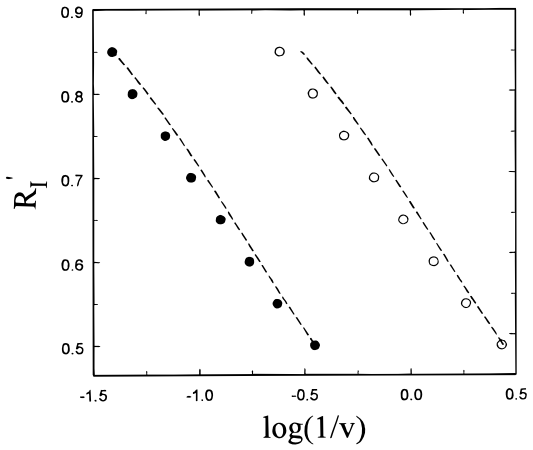

Figure 1. Experimental DCV data for the reactions of DMA$^{\bullet+}$ (○) and DMA-$d_6^{\bullet+}$ (●) with LUT as a function of voltage sweep rate. $[DMA]_o = 2.0$ mM, $[LUT]_o = 4.0$ mM. The dashed lines are theoretical data for a simple second-order proton-transfer reaction with $k_{app} = 4820$ M^{-1} s^{-1} (DMA$^{\bullet+}$) and 650 M^{-1} s^{-1} (DMA-$d_6^{\bullet+}$).

Table 1. Kinetic Data for the Reaction between DMA$^{\bullet+}$ and DMA-$d_6^{\bullet+}$ with DPP and LUT in Dichloromethane−Bu_4NPF_6 (0.2 M)[a]

	DPP (50 mM)[b]			LUT (4.0 mM)[c]		
R'_I	ν_H (V/s)[d]	ν_D (V/s)[d]	KIE_{app}	ν_H (V/s)[d]	ν_D (V/s)[d]	KIE_{app}
0.85	47.5	4.02	11.8	25.6	4.13	6.21
0.80	34.0	2.78	12.2	20.5	2.87	7.13
0.75	25.0	1.97	12.7	14.4	2.05	7.01
0.70	19.5	1.50	13.0	10.9	1.48	7.34
0.65	15.2	1.11	13.7	7.90	1.08	7.31
0.60	11.6	0.852	13.7	5.78	0.778	7.41
0.55	8.88	0.615	14.3	4.26	0.547	7.75
0.50	6.87	0.470	14.6	2.82	0.369	7.62

[a] DCV measurements at 291 K. [b] Substrate concentration 1.0 mM. [c] Substrate concentration 2.0 mM. [d] Each data point obtained from 18 to 60 voltammograms.

Table 2. Kinetic Data for the Reaction between MPA$^{\bullet+}$ and MPA-$d_3^{\bullet+}$ with DPP and LUT in Dichloromethane−Bu_4NPF_6 (0.2 M)[a]

	DPP (50 mM)[b]			LUT (2.0 mM)[b]		
R'_I	ν_H (V/s)[c]	ν_D (V/s)[c]	KIE_{app}	ν_H (V/s)[c]	ν_D (V/s)[c]	KIE_{app}
0.85	36.9	4.24	8.7	13.5	2.54	5.3
0.80	27.2	2.72	10.0	9.27	1.68	5.5
0.75	21.6	1.92	11.2	6.72	1.09	6.2
0.70	16.7	1.49	11.2	5.04	0.816	6.2
0.65	12.1	1.09	11.1	3.85	0.577	6.7
0.60	9.59	0.850	11.3	2.94	0.433	6.8
0.55	7.70	0.653	11.8	2.08	0.293	7.1
0.50	5.53	0.470	11.8	1.43	0.195	7.3

[a] DCV measurements at 291 K. [b] Substrate concentration 1.0 mM. [c] Each data point obtained from 18 to 60 voltammograms.

(12) Reitstøen, B.; Parker, V. D. *J. Am. Chem. Soc.* **1990**, *112*, 4968; Xue, J.-Y.; Parker, V. D. *J. Org. Chem.* **1994**, *59*, 6564.
(13) Parker, V. D.; Chao, Y.-T.; Zheng, G. *J. Am. Chem. Soc.* **1997**, *119*, 11390.
(14) Chao, Y.-T. Master of Science Thesis, Utah State University: Logan, VT, 1993.
(15) Parker, V. D. *Electroanal. Chem.* **1983**, *19*, 131; Ahlberg, E.; Parker, V. D. *J. Electroanal. Chem.* **1981**, *121*, 57.
(16) Bard, A. J.; Faulkner, L. *Electrochemical Methods*; Wiley: New York, 1980.
(17) Reitstøen, B.; Norrsell, F.; Parker, V. D. *J. Am. Chem. Soc.* **1989**, *111*, 8463; Parker, V. D.; Reitstøen, B.; Tilset, M. *J. Phys. Org. Chem.* **1989**, *2*, 580; Reitstøen, B.; Parker, V. D. *J. Am. Chem. Soc.* **1991**, *113*, 6954; Parker, V. D.; Handoo, K. L.; Reitstøen, B. *J. Am. Chem. Soc.* **1991**, *113*, 6218; Parker, V. D.; Tilset, M. *J. Am. Chem. Soc.* **1991**, *113*, 8778.
(18) Rudolph, M.; Reddy, D. P.; Feldberg, S. W. *Anal. Chem.* **1994**, *66*, 589A and references therein.

Table 3. Apparent Second-Order Rate Constants[a] for Radical Cation Proton-Transfer Reactions

reactants	k_{app}^{H} (M^{-1} s^{-1})	k_{app}^{D} (M^{-1} s^{-1})
$DMA^{\bullet+}$/DPP	601	44.3
$DMA^{\bullet+}$/LUT	4820	650
$MPA^{\bullet+}$/DPP	485	44.0
$MPA^{\bullet+}$/LUT	4688	651

[a] Calculated from $R'_I = 0.50$ data.

Table 4. Apparent and Real Deuterium Kinetic Isotope Effects under Steady-State Conditions[a]

k_p^H/k_b	1000	100	10	1.0	0.1	0.01
KIE_{app}/KIE_{real}	0.011	0.0198	0.10	0.505	0.91	0.99

[a] For reactions following eq 1, calculated from $KIE_{app} = KIE_{real}(k_b + k_p^D)/(k_b + k_p^H)$.

to R'_I), and can be equated to the real kinetic isotope effect (KIE_{real}) for the proton transfer.

The data, however, suggest a complex mechanism, such that k_{app} values, and hence KIE_{app} values, approach the steady-state values as the extent of reaction increases. The obvious hypothesis developed at this stage of our study, supported by indirect evidence from previous studies,[12,13] is that the proton-transfer reactions between the methylarene radical cations and the nitrogen-centered bases follow a general mechanism (eq 1) in which all three rate constants (k_f, k_b, and k_p) contribute to the overall rate of the reaction. Furthermore, the variation of KIE_{app} with decreasing R'_I suggests that the reactions do not reach steady-state until R'_I is approaching 0.5. Preliminary digital simulation of the mechanism (eqs 3−5) verified that with the proper selection of the rate constants, theoretical data could be generated that closely mimicked the experimental data.

$$ArCH_3^{\bullet+} + B \rightleftarrows ArCH_3^{\bullet+}/B \; K_3 k_f/k_b \qquad (3)$$

$$ArCH_3^{\bullet+}/B \rightarrow ArCH_2^{\bullet} + BH^+ k_p \qquad (4)$$

$$ArCH_2^{\bullet} + ArCH_3^{\bullet+} + B \rightarrow \text{products} \quad \text{fast} \qquad (5)$$

Apparent and Real Deuterium Kinetic Isotope Effects for Proton-Transfer Reactions. Application of the steady-state approximation on HA/B (eq 1) results in the rate law (eq 6),

$$\text{rate} = k_{app}[HA][B] \qquad (6)$$

$$KIE_{app} = KIE_{real}(k_b + k_p^D)/(k_b + k_p^H) \qquad (7)$$

and the apparent rate constant (k_{app}) is equal to $k_f k_p/(k_b + k_p)$. This gives rise to an expression (eq 7) to relate KIE_{app} to KIE_{real} (equal to k_p^H/k_p^D). The data in Table 4 illustrate the effect of k_p^H/k_b on KIE_{app}/KIE_{real} when holding k_f equal to k_b. An important consequence of eq 7 is that under steady-state conditions, that is, those under which the rate law (eq 6) is applicable, KIE_{app} are constants independent of the extent of reaction. However, the data in Table 4 show that KIE_{app} cannot necessarily be equated to KIE_{real}, even under steady-state conditions; rather, KIE_{app}/KIE_{real} varies with k_p^H/k_b from 0.011 to 0.99 for a 10^5-fold change in the ratio in the range given.

Since the steady-state apparent rate constants, $(k_{app}^H)_{s.s.}$ and $(k_{app}^D)_{s.s.}$ (eqs 8 and 9), are available from the kinetic studies,

$$(k_{app}^H)_{s.s.}/k_f = (k_p^H/k_b)/(1 + k_p^H/k_b) = CH \qquad (8)$$

$$(k_{app}^D)_{s.s.}/k_f = (k_p^D/k_b)/(1 + k_p^D/k_b) = CD \qquad (9)$$

let us relate these quantities to the kinetic isotope effects. From eqs 8 and 9 we have $k_p^H/k_b = CH/(1 - CH)$ and $k_p^D/k_b = CD/(1 - CD)$. The value of the real kinetic isotope effects is then given by eq 10. Thus, in addition to the apparent rate constants,

$$KIE_{real} = [CH/(1 - CH)]/[CD/(1 - CD)] \qquad (10)$$

it is necessary only to determine k_f in order to evaluate KIE_{real}.

The lower limit of k_f is $(k_{app}^H)_{s.s.}$, since the right-hand side of eq 8 can approach but cannot exceed unity as k_p^H/k_b becomes large. The practical upper limit of k_f where the reaction rate still depends on k_p^H/k_b, is when this ratio is equal to <0.1. Thus, apparently it is feasible to resolve the rate constants in the proton-transfer mechanism only under non-steady-state conditions and where k_f falls in the range between $(k_{app}^H)_{s.s.}$ and $11(k_{app}^H)_{s.s.}$.

Fitting Experimental DCV Data to Theoretical Data Obtained by Digital Simlulation. For a simple second-order proton-transfer reaction between a radical cation and a base, theoretically the slope of the R'_I vs ν^{-1} response curve is independent of the second-order rate constant and KIE_{app} are independent of R'_I. Obviously, the experimental data in Tables 1 and 2 do not conform to this mechanism. On the other hand, each of the eight sets of data in Tables 1 and 2 can be readily fit to theoretical data for the complex mechanism (eqs 3−5), keeping the individual rate constants consistent with the appropriate k_{app} (Table 3). However, the experimental to theoretical data fit is not unique when a single response curve is considered. Generally, several combinations of rate constants will give an acceptable data fit.

The concurrent fitting of data for both $ArCH_3^{\bullet+}$ and $ArCD_3^{\bullet+}$ results in a unique set of rate constants that gives the best correspondence between the experimental response and the theoretical data.[19] To arrive at this unique set of rate constants, the parameters must be varied over a wide range in a systematically. Arriving at the unique set of rate constants requires a large number of simulations.

Our data-fitting procedure involves calculating $(\nu_{exp}^H - \nu_{sim}^H)^2/\nu_{sim}^H$, $(\nu_{exp}^D - \nu_{sim}^D)^2/\nu_{sim}^D$, and $(KIE_{exp} - KIE_{sim})^2/KIE_{sim}$, where ν^H and ν^D are the voltage sweep rates necessary for a particular R'_I and the subscripts refer to experimental (exp) and simulation (sim) data. The calculations are made at each R'_I from 0.85 down to 0.50 and each of these is summed over the entire range ($\sum_H$, $\sum_D$, and $\sum_{KIE}$). Since the dependence of KIE_{app} on R'_I is the most important parameter in arriving at a unique fit, $\sum_{KIE}$ is used directly in the data fit, while $\sum_H$ and $\sum_D$ are monitored to ensure that good fits to the two response curves are obtained.

The fact that the range of k_f over which R'_I-dependent KIE_{app} are expected to be observed is limited [i.e. from k_{app}^H to $11(k_{app}^H)$] suggests what strategy to follow. We typically select about 10 k_f values over the applicable range, starting at $1.1(k_{app}^H)$, and determine what values of the other rate constants, k_p^H, k_b, and k_p^D, give the best fit for that particular k_f value. This is done by varying k_p^H and adjusting (k_b and k_p^D) to conform to eqs 8−10. For each k_f, a series of $\sum_{KIE}$ as a function of k_p^H is obtained. Plots of $\sum_{KIE}$ vs k_p^H are parabola-like curves

(19) In numerous cases we have used theoretical instead of experimental data as the known input to challenge our ability to assign unknown rate constants with k_{app}^H, k_{app}^D, and R'_I-dependent KIE_{app} as the "experimental" data, using the concurrent fitting of DCV data for reactions of HA and DA and the procedure described here. We have, in all cases where k_f ranges from $1.1(k_{app}^H)$ to $11(k_{app}^H)$, been able to precisely identify k_f, k_b, k_pH, and k_p^D. On the other hand, when theoretical R'_I vs ν^{-1} data are used to attempt to assign rate constants based only on a single response curve (reactions of either HA or DA), several alternative sets of rate constants are observed to give acceptable fits of the data.

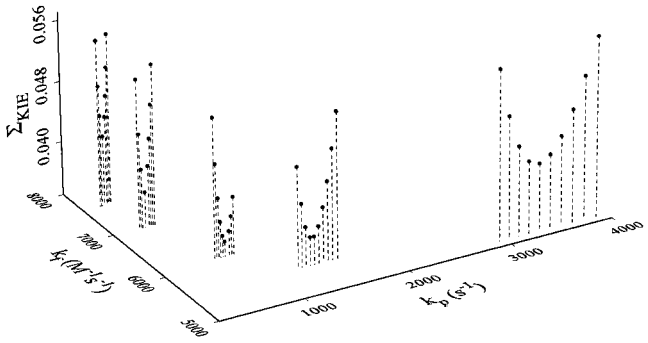

Figure 2. Three-dimensional least-squares analysis for the reaction of $DMA^{\bullet+}$ with LUT. For the sake of clarity, the data shown are only a fraction of the total used in the analysis. Rate constant assignment: $k_f = 6120\ M^{-1}\ s^{-1}$ and $k_p^H = 817\ s^{-1}$.

Table 5. Electron-Transfer Rate Constants for Reduction Reactions[a]

complex	$K_3(M^{-1})$[b]	$\Delta E^o(mV)$[c]	K_{et}[d]	$k_{et}(M^{-1}\ s^{-1})$[e]
$MPA^{\bullet+}$/DPP	2.83	3.3	0.88	8 300
$MPA^{\bullet+}$/LUT	74.4	3.7	0.86	14 000
$DMA^{\bullet+}$/DPP	2.10	2.5	0.91	<5 000
$DMA^{\bullet+}$/LUT	25.2	2.4	0.92	<5 000

[a] See text for description of rate constant assignments. [b] Evaluated from k_f and k_b for complex formation. [c] Calculated from eq 12: $\Delta E^o = E^o(ArCH_3^{\bullet+}/ArCH_3) - E^o(complex^{\bullet+}/complex)$. [d] Equilibrium constant for reaction 13. [e] Forward rate constant for reaction 13.

with minima that reflect the best fit of experimental to theoretical data for the k_f value. The overall result is a series of the fitting parameter at the minimum, $(\sum_{KIE})_{min}$, as a function of k_f.

A plot of $(\sum_{KIE})_{min}$ vs k_f is, again, parabola-like with a minimum that reflects the best value of k_f.

The fitting procedure is demonstrated graphically in Figure 2, which plots k_p on the *x*-axis, k_f on the *y*-axis and $\sum_{KIE}$ on the *z*-axis. Each of the five parabola like curves projected onto the x−z plane give the dependence of $\sum_{KIE}$ on k_p at the particular value of k_f. The minima of the five curves when projected in the *y*−*z* plane are used to define the best fit of experimental to theoretical data for k_f, which is assigned the value at the minimum of this curve.

The procedure described to this point is the first iteration for estimating the rate constants. It is then necessary to refine the data in the regions of the minima to obtain high resolution of the data fit.

For each k_p used at each k_f it is necessary to carry out ∼30 simulations (15 for HA and 15 for DA) to generate the R'_I vs ν^{-1} response curves for HA and DA. The first iteration of fitting usually involves ∼25 k_p^H at 10 k_f, which requires ∼7500 simulations to gather the necessary theoretical data. This is followed by further refinements, including the electron-transfer reaction discussed in the following section. On the order of 10 000 or more simulations were carried out for each system studied. Details of the simulation procedure are given in the *Experimental Section*.

Homogeneous Electron-Transfer Reactions during the Reverse Cyclic Voltammetry Scan. The equilibrium constants (K_3) for the radical cation−base reactions (eq 3) studied here are moderate (Table 5). This implies that the complexes, $ArCH_3^{\bullet+}$/B, will have reduction potentials (reaction 11) not very different from those of the parent radical cations. The effect of K_3 on $E°$ for charge-transfer reaction 11 is given by eq 12,[20,21] where $\Delta E°$ is the difference in electrode potential for reduction of the radical cations as compared with the corresponding complexes. In all four cases $\Delta E°$, calculated with eq 12, was <4 mV (Table 5). The fact that the second-order rate constants for formation of the complexes (discussed in the following sections and summarized later in Table 7) are relatively small suggests that the homogeneous electron-transfer reactions (reaction 13) will be of greater importance than diffusion of the

$$ArCH_3^{\bullet+}/B + e^- \rightarrow ArCH_3/B \quad (11)$$

$$\Delta E° = (2.303RT/F)\log(1 + K_3[B]) \quad (12)$$

$$ArCH_3^{\bullet+}/B + ArCH_3 \rightleftarrows ArCH_3/B + ArCH_3^{\bullet+} \quad (13)$$

$$ArCH_3/B \rightarrow ArCH_3 + B \quad (14)$$

$$\log K_{13} = F\Delta E°/2.303RT \quad (15)$$

$$ArCH_3^{\bullet+}/B \rightarrow ArCH_3^{\bullet+} + B \quad (16)$$

complex to the electrode and charge-transfer reaction 11. Reaction 13 is expected to be accompanied by the very rapid dissociation of the neutral complexes (reaction 14). The equilibrium constants for reactions 13 and 14 are readily calculated (eq 15). Since $ArCH_3$ is consumed in reaction 13 and regenerated in reaction 14, the overall effect of these two reactions is reaction 16, which is identical to reverse reaction 3. Thus reactions 13 and 14, although they do not contribute to the rate determining steps, will affect the DCV data and must be taken into account in the simulations.

The source of radical cation in the reduction of $ArCH_3^{\bullet+}$ at the electrode during the cyclic voltammetry reduction scan is not only reactions 13 and 14 but also equilibrium 3, which is drawn to the left by the depletion of $ArCH_3^{\bullet+}$ in the reaction layer. The latter has already been accounted for in the simulation iterations described in the previous section. Reactions 13 and 14 were readily taken into account by treating 13 as an irreversible reaction followed by a very rapid 14. Further iterations in the simulations were carried out in which k_{13} was varied to give the best fit of experimental to theoretical DCV data. The last column in Table 5 gives the values of k_{13} obtained from the fitting procedure. Improvements in the data fits were observed when reactions 13 and 14 were included for the reactions of $MPA^{\bullet+}$ but little effect was observed for those of $DMA^{\bullet+}$. In all cases, including these reactions caused only a minor perturbation in the simulated DCV response for the proton-transfer reactions.

Since our primary interest is in the proton-transfer reactions of the radical cations, we have evaluated only the rate constants for reaction 13 in connection with gaining the best fit of experimental and theoretical data for the DCV response. No attempt was made to study the details of the electron-transfer reactions.

Uncertainty in Rate Constant and KIE_{real} Assignments. The experimental error in the determination of R'_I values was observed to be on the order of ±0.004, which corresponds <1% in the range where R'_I equals 0.5 to 0.85. However, the experimental error is not the primary source of the uncertainty in assignment of microscopic rate constants. The data in Table 6 show that the error in KIE_{real} has a marked dependence on k_f/k_{app}^H. When this ratio is close to unity, even a 1% error in k_f gives rise to a very large error in KIE_{real}. At the other extreme,

(20) Shifts in reversible electrode potentials have been used to determine equilibrium constants for a number of reactions following charge transfer (see ref 21 and literature cited therein).

(21) Parker, V. D. *Acta Chem. Scand.* **1984**, *B-38*, 125, 189, 741; Peover, M. E.; Davies, J. D. *J. Electroanal. Chem.* **1963**, *6*, 46.

Table 6. Error in Real Kinetic Isotope Effects as a Function of k_f/k_{app}^{H}[a]

k_f/k_{app}^{H}	k_f (M^{-1} s^{-1})	KIE_{real}	range (±1% error in k_f)
1.02	4916	328	220−693
1.05	5061	135	113−170
1.10	5390	61.5	56.8−67.1
1.20	5784	39.4	37.5−41.4
1.50	7230	20.2	19.8−20.6
2.00	9640	13.8	13.7−13.9
5.00	24100	8.99	8.97−9.01

[a] Assumes k_{app}^{H} equal to 4820 and k_{app}^{D} equal to 652.

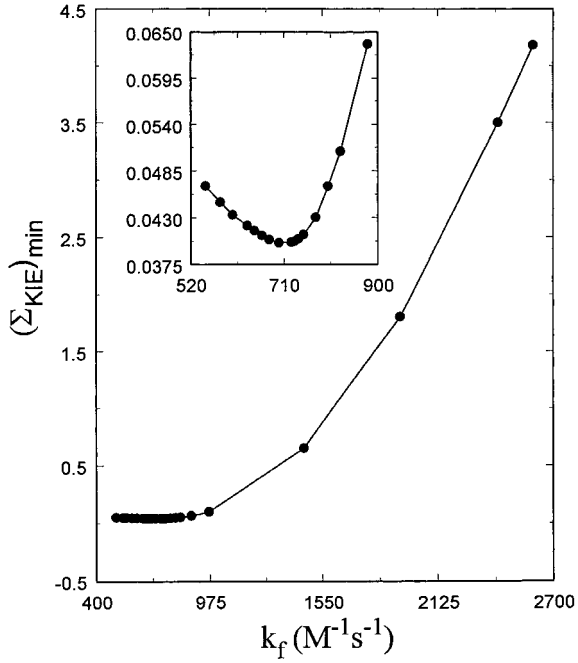

Figure 3. Fitting procedure applied to the reaction between $MPA^{\bullet+}$ and DPP in dichloromethane-$Bu_4N^+PF_6^-$ (0.2 M) at 291 K. [MPA] = 1.0 mM, [DPP] = 50 mM.

for $k_f/k_{app}^{H} = 5$, a 1% error in k_f gives rise to only a negligible error in KIE_{real}. This relation must be kept in mind when assessing errors.

Rate Constant Assignments for the Reactions of Methylarene Radical Cations with Pyridine Bases. The results of the fitting procedure used to assign rate constants to the radical cation−base reactions are summarized in Figure 3 and in the Supporting Information (Figures S1−S3). The $(\Sigma_{KIE})_{min}$ vs k_f data, obtained from the 3-dimensional analysis presented earlier, are indicated for k_f values ranging from k_{app}^{H} to $>5(k_{app}^{H})$. The inserts in the figures are the expanded-scale plots in the region where the minimum, if observed, occurs. The interpretation for the analysis for the reactions of $MPA^{\bullet+}$ with both LUT (Figure S1) and DPP (Figure 3), as well as that for $DMA^{\bullet+}$ with LUT (Figure S2), are straightforward and the rate constants calculated at the minima of the $(\Sigma_{KIE})_{min}$ vs k_f plots are assigned. These are summarized in Table 7.

On the other hand, $(\Sigma_{KIE})_{min}$ for the reaction between $DMA^{\bullet+}$ and DPP (Figure S3) steadily increases as k_f increases throughout the applicable range of k_f. We cannot assign unique rate constants in this case since the required minimum was not observed. Even in this case, minima were observed in all of the Σ_{KIE} vs k_p^{H} plots at constant k_f (i.e. the dimension perpendicular to the $(\Sigma_{KIE})_{min}$ vs k_f plane of Figure S3). Our conclusion is that in this case k_f is too close to k_{app} to allow observation of the minimum. We confirmed by simulations for $k_f = 1.05(k_{app}^{H})$ that a minimum is not expected under these conditions and we did not observe an experimentally significant minimum under these conditions. Significant minima are observed with $k_f > 1.1(k_{app}^{H})$, which places k_f in the region between k_{app} and $1.1(k_{app}^{H})$ and justifies our assignment of $k_f = 1.05\ (\pm 0.05)(k_{app}^{H})$. We did not include rate constant assignments for the $DMA^{\bullet+}$/DPP reaction in Table 7 since we were unable to assign a unique set of rate constants in this case and our assignment of $k_f = 1.05(\pm 0.05)(k_{app}^{H})$ gave rise to very large errors in the other rate constants and in KIE_{real} (see Table 6).

Since the proton-transfer reactions involve the abstraction of a proton from $-CH_3$ and $-CD_3$, the KIE are the product of the primary KIE for cleavage of the C−H(D) bond and the α-secondary KIE.[22] α-Secondary KIE are typically on the order of 1.15 per deuterium atom.[23] This suggests that the primary KIE for the proton-transfer reactions are on the order of 0.76 times the total KIE.

Protonated pyridines (BH^+) probably also take part in equilibrium 17, at least to some extent, in dichloromethane−Bu_4NPF_6 (0.2 M). If the equilibrium constant (K_{17}) is sufficiently

$$BH^+ + B \rightleftarrows BHB^+ \qquad (17)$$

large, this will affect [B] in the reaction layer. The nitrogen centers in DPP and LUT are crowded because of the bulky 2,6-substituents, which makes formation of BHB^+ somewhat unfavorable. Reaction 17, regardless of the magnitude of K_{17}, is not expected to have any effect on the kinetics of the reactions studied under pseudo first-order conditions (B = DPP) but a large K_{17} would affect the reactions involving LUT under second-order conditions. Including reaction 17 with a large K_{17} in simulations had little effect on Σ_{KIE} but gave significantly larger values of Σ_{HA} and Σ_{DA} for both reactions involving LUT, thus indicating a less satisfactory comparison between experimental and theoretical data. Since the reactions of HA and DA are studied at the same extent of reaction, the relative effect of equilibrium 17 should be the same in both reactions and have a minimal effect on the magnitude of KIE_{app}—which is consistent with the insensitivity of Σ_{KIE} to the change in conditions.

Digital simulations were carried out to determine whether incompletely labeled substrate could be responsible for the observation of extent-of-reaction-dependent KIE_{app}. The Grignard reaction with methyl-d_3-iodide (99.5+%) is expected to yield 9-methyl-d_3-10-phenylanthracene of the same isotopic purity. Simulations according to a simple proton-transfer mechanism of the reactions of MPA and MPA-$d_3^{\bullet+}$ (98.5%)/MPA-$d_2^{\bullet+}$ (1.5%) with DPP and LUT in which no KIE was assumed for the reaction of MPA-$d_2^{\bullet+}$ failed to reveal extent-of-reaction-dependent KIE.

Discussion

Once steady-state is achieved, the rate law (eq 6) applies to proton-transfer reactions following general mechanism 1, and k_{app} cannot be resolved into the individual contributions of k_f, k_b, and k_p. On the other hand, during the period before steady-state is reached, the various rate constants affect the overall reaction rate to different degrees than those implied by the rate law (eq 6). Provided that k_p^{H}/k_b falls in the range from ~0.1 to 1000, the possibility of resolving the kinetics exists. Under these conditions, the relative effects of k_p^{H} and k_p^{D} differ during the non-steady-state period, and the KIE_{app} values dependent on the

(22) Streitweiser, A.; Jagow, R. H.; Fahey, R. C.; Susuki, S. *J. Am. Chem. Soc.* **1958**, *80*, 2326.

(23) Carrol, F. A. *Perspectives on Structure and Mechanism in Organic Chemistry*; Brooks/Cole: Pacific Grove, CA, 1998.

Table 7. Rate Constants and Kinetic Isotope Effects for Proton-Transfer Reactions[a]

R.C. (mM)[b]	base (mM)[c]	k_f (M^{-1} s^{-1})	k_b (s^{-1})	k_p^H (s^{-1})	KIE_{app}	KIE_{real}
$MPA^{\bullet+}$(1.0)	LUT (2.0)	5300	67.6	518	5.3−7.3	47
$MPA^{\bullet+}$(1.0)	DPP (50)	707	250	545	8.7−11.8	33
$DMA^{\bullet+}$(2.0)	LUT (4.0)	6120	244	817	6.2−7.8	31

[a] Reactions in dichloromethane-Bu_4NPF_6 (0.2 M) at 291 K. [b] Radical cation, substrate concentrations in parentheses. [c] Base concentrations in parentheses.

extent of reaction are predicted by theory (simulation). The latter provide an effective means of comparing experimental with theoretical data and allows the assignment of unique sets of rate constants for the proton-transfer reactions. We have experimentally observed this behavior during kinetic studies of the proton-transfer reactions of methylarene radical cations with pyridine bases.

The kinetic data for the proton-transfer reactions are summarized in Table 7. The forward rate constants (k_f) for the formation of radical cation−base complexes are 8−10 times greater when the base is LUT than for DPP. On the other hand, the limited data are not conclusive with regard to the effect of structure on the magnitude of the other two rate constants. All of the KIE_{real}, taking into account the expected α-secondary KIE, are clearly out of the range expected for classical KIE and implicate the occurrence of quantum mechanical tunneling.[24−27] Further studies on all of these reactions are needed to determine the temperature effect on k_p^H and k_p^D and to gain more knowledge on proton tunneling in these systems.

As was pointed out earlier, the proton-transfer kinetics for mechanism 1 can be resolved only when k_p^H/k_b falls in a rather limited range. If k_{app} for the 2-step mechanism is moderate and the encounter complexes are formed at diffusion-controlled rates, the reaction kinetics cannot be resolved. For the proton-transfer reactions of methylarene radical cations with pyridine bases, the complexes involved in mechanism 1 cannot be the encounter complexes that form at every collision. On the other hand, previous studies[12,13,17] have evidence that both proton-transfer reactions and nucleophile-combination reactions of the radical cations pass through kinetically significant intermediates, which have been proposed to be π-complexes between the radical cations and the nitrogen-centered bases (nucleophiles). The detailed structure of these complexes is unknown and perhaps further studies in which the proton-transfer kinetics are resolved will provide indirect evidence of structure.

The data in Table 4 indicate that for proton-transfer mechanism 1 in the dynamic range between limiting rate laws, where k_{app} corresponds to neither k_f nor k_pK_{eq}, KIE_{app} differ significantly from KIE_{real}. For this mechanism these terms are identical only under conditions where $k_{app} = k_pK_{eq}$, that is, conditions under which the preequilibrium is rapidly established before slower proton transfer takes place. The observation of extent-of-reaction-dependent KIE_{app} during the stage of the reaction before steady-state is established thus provides evidence that the experimental conditions correspond to the dynamic range between the limiting rate laws. It is well-known that reactions having multiple rate-limiting steps can give rise to KIE_{app} that cannot be equated to KIE_{real} (often called the intrinsic isotope effect in enzyme reactions).[28]

The experimental data reported here show the characteristic feature of KIE_{app} which vary with extent of reaction, thus indicating that the data are obtained under non-steady-state conditions where the rate law (eq 6) is not applicable. The data presented (Tables 1−3 and Figures 1−3, S1−S3) clearly demonstrate that the fitting of experimental to theoretical data for mechanism 1 provides a means to resolve k_{app} into the microscopic rate constants k_f, k_b, and k_p.

Kinetic studies carried out under steady-state conditions where the rate law (eq 6) applies clearly leave considerable uncertainty in the significance of the observed KIE. One would need to resolve k_{app} (eq 6) and evaluate the microscopic rate constants (k_f, k_b, k_p^H, and k_p^D) to have any confidence that deuterium KIE_{app} could be equated to KIE_{real}. It seems highly likely that proton-transfer reactions of many different classes of carbon acids, including organic radical cations other than those studied here, fall in the dynamic range where KIE_{app} are only a fraction of KIE_{real}. Should this be the case, the KIE reported for these reactions may only be fractions of KIE_{real}. Further studies in which proton-transfer kinetics are resolved are necessary to answer this question.

Aside from the intrinsic interest in the phenomenon of tunneling during proton-transfer reactions, there are other important reasons to know the magnitude of the effect. The magnitude of the deuterium KIE is often used in the description of transition states for proton transfer, for example, as in the discussion of the variation of deuterium KIE as a function of acid strength of AH and BH^+, wherein bell-shaped curve is often obtained when KIE are plotted vs pK_a of BH^+ for the proton-transfer reaction of AH with B. A common explanation of this phenomenon, attributed to Westheimer,[29] is that the maximum occurs when the proton is bonded equally to A^- and B in the transition state. On the other hand, the explanation of Bell et al.[30] is that maxima are found when HA and BH^+ are of equal strength, under which conditions quantum mechanical tunneling is expected to be maximal. Regardless of which interpretation is correct, neither will be valid unless the KIE values used in the correlation are real rather than apparent values.

It is of interest to note that most of the clearly documented cases[31] of large k_H/k_D values attributable to hydrogen tunneling are for unimolecular reactions,[32] including rearrangement of sterically hindered aryl radicals,[33] *enol*−ketone transformation

(24) Bell, R. P. *The Tunnel Effect in Chemistry*; (Chapman & Hall: London, 1980).

(25) Siebrand, W.; Wildman, T. A.; Zgierski, M. Z. *J. Am. Chem. Soc.* **1984**, *106*, 4083.

(26) There have been many more recent advances in the dynamics of proton transfer and proton tunneling and the introductory[27] and subsequent papers in an issue of the *Deutsche Berichte Bunsen-Gesellschaft fur Physikalische Chemie* devoted to "Hydrogen Transfer: Theory and Experiment" provide ready access to this literature.

(27) Limbach, H.-H.; Manz, J. *Ber. Bunsen-Ges. Phys. Chem.* **1998**, *102*, 289.

(28) Melander, L.; Saunders, W. H. Reaction Rates of Isotopic Molecules; John Wiley: New York, 1980; pp 158−162. Cleland, W. W. *Bioorg. Chem.* **1987**, *15*, 283. Sinnott, M.; Garner, C. D.; First, E.; Davies, G. *Comprehensive Biological Catalysis, A Mechanistic Reference*; Academic Press: San Diego, 1998; Vol. 4, pp 47−58, and references therein.

(29) Westheimer, F. H. *Chem. Rev.* **1961**, *61*, 265.

(30) Bell, R. P.; Sachs, W. H.; Tranter, R. L. *Trans. Faraday Soc.* **1967**, *67*, 1995.

(31) The examples of hydrogen tunneling presented are not the most recent ones and were chosen on the basis of the magnitude of KIE.

(32) Siebrand, W.; Wildman, T. A.; Zgierski, M. Z. *J. Am. Chem. Soc.* **1984**, *106*, 4089.

(33) Brunton, G.; Gray, J. A.; Griller, D.; Barclay, L. R. C.; Ingold, K. U. *J. Am. Chem. Soc.* **1978**, *100*, 4197.

of 2-methylacetophenone,[34] a sigmatropic hydrogen shift in hexahydrocarbazole,[35] and intramolecular hydrogen migration between nitrogen atoms of *meso*-tetraphenylporphine.[36] For unimolecular reactions, KIE_{app}, which are not necessarily equal to KIE_{real}, are not expected to depend on the extent of reaction. Two examples of large KIE reported for proton-transfer reactions include proton transfer to benzene anion in ethanol ($k_H/k_D = 100$ at 77 K)[37] and proton transfer in naphthol/ammonia complexes ($k_H/k_D > 200$ at 10 K).[38]

Hydrogen tunneling in biochemical systems has recently been observed in a number of cases and is of intense current interest.[39] A pertinent example is the hydrogen atom abstraction from linoleic acid by soybean lipoxygenase,[40,41] a reaction in which both hydrogen and deuterium tunneling have been found.[42] But it is not clear whether the KIE reported in these studies are apparent or real values.

The observation of very large k_H/k_D during proton-transfer reactions of 4-nitrophenylnitromethane with amine bases[43] was attributed to extensive tunneling and served as strong evidence for the phenomenon. Several later investigations[44] showed that the KIE were actually normal and that the observation of the large KIE_{app} was an artifact that could be attributed to kinetic deviations caused by the exchange of D in the labeled substrate with amino H and adventitious water. Could a similar artifact be responsible for the large KIE observed in the present study? We do not believe that exchange of D in the labeled radical cation is feasible. We know of no instances where methylarene radical cations undergo exchange of methyl H or D. In fact, the abstractions of H and D from the methyl group are thermodynamically favorable reactions followed by rapid electron transfer from the resulting radical to generate the carbenium ion.

We also considered the presence of isotopic impurities in the radical cations as a possible source of the extent-of-reaction-dependent KIE_{app}. Simulation results for KIE studies of the reactions of $MPA^{\bullet+}$ and MPA-$d_3^{\bullet+}$ contaminated with 1.5% of MPA-$d_2^{\bullet+}$, in which the latter was assumed to react at the same rate as $MPA^{\bullet+}$, failed to predict extent-of-reaction-dependent KIE_{app}. Furthermore, if the observation of extent-of-reaction-dependent KIE_{app} were due to isotopic impurities, the effect would be expected to be as much as 2 times greater for the reactions of DMA-$d_6^{\bullet+}$ than for those of MPA-$d_3^{\bullet+}$. The experimental results show the opposite trend: KIE_{app} for the reactions of $DMA^{\bullet+}$ increased by factors of ~1.23 in the range $R'_I = 0.85-0.50$, whereas those for the corresponding increases for $MPA^{\bullet+}$ were ~1.37.

Our results show that KIE_{app} during proton-transfer reactions can be far less than KIE_{real}, which suggests the distinct possibility that the magnitude of KIE_{real} and hence the influence of proton tunneling in these reactions can be much greater than previously realized. Our successful resolution of the four pertinent rate constants (k_f, k_b, k_p^H, and k_p^D) for microscopic reaction steps during the proton transfer reactions of methylarene radical cations suggests that the approach may be applicable in other cases and has the potential to greatly enrich the fundamental knowledge of proton-transfer reactions.

Experimental Section

Materials. Dichloromethane was allowed to reflux for several hours over $CaCl_2$ and, after passing through active neutral alumina, was used without further purification. Bu_4NPF_6 (Aldrich) was recrystallized from dichloromethane−ether before use. DMA (Aldrich) was recrystallized from 2-propanol before use. MPA was obtained from bromination of 9-phenylanthracene in CCl_4, followed by halogen−lithium exchange with *tert*-butyllithium under an argon atmosphere and reaction with methyl iodide in tetrahydrofuran at −78 °C. 9-Methyl-d_3-10-phenylanthracene was prepared in the same way, with use of methyl-d_3-iodide (99.5+%) as alkylating agent. 9,10-Dimethyl-d_6-anthracene was prepared according to the method of Fieser and Heymann[45] with methyl-d_3-magnesium iodide (99.5+%) used as the Grignard reagent. 2,6-Dimethylpyridine (99+%, Aldrich) was distilled under reduced pressure before use. DPP from Aldrich was recrystallized from 2-propanol−petroleum ether. We observed differences between the rate constants determined with recrystallized DPP and with that used as received.

Instrumentation and Data Handling Procedures. Cyclic voltammetry was performed with a Princeton Applied Research (Princeton, NJ) Model 173 potentiostat/galvanostat driven by a Hewlett-Packard 3314A function generator. After passing through a dual-channel low-pass filter (Stanford Research Systems, Inc., Model SR640), the data were recorded on a Nicolet Model 310 digital oscilloscope with 12-bit resolution. The oscilloscope and function generator were controlled by a personal computer via an IEEE interface.

The current−potential curves were collected at selected trigger intervals to reduce periodic noise,[46] and 3 or more curves were averaged before treating with a frequency domain low pass digital filter and numerical differentiation. The standard deviation in R'_I obtained this way was ±0.004.

Cyclic Voltammetry Measurements. A standard 3-electrode 1-compartment cell was used for all kinetic measurements. Positive-feedback IR compensation was used to minimize the effects of uncompensated solution resistance. Reference electrodes were $Ag/AgNO_3$ (0.01 M) in acetonitrile constructed as described by Moe.[47] The working electrodes, 0.2−0.8 mm Pt, were prepared by sealing wire in glass and polishing to a planar surface as described previously.[48] The working electrodes were cleaned before each series of measurements with a fine polishing powder (Struers, OP−Alumina Suspension) and wiped with a soft cloth. The cell was immersed in a water bath controlled to 18 ± 0.2 °C.

Kinetic Measurements. Rate constants were obtained by comparing DCV[15] data with the theoretical data obtained by digital simulation.[16] The reactions were studied both under pseudo-first-order and second-order conditions and using solutions (CH_2Cl_2/0.2 M Bu_4NPF_6) containing substrate (1.0−2.0 mM) and base (0.5−50 mM) at 291 K. The experimental R'_I data were adjusted to 0.05 intervals in the range 0.85 to 0.50 by linear log−log interpolation. (We have previously observed that log R'_I vs log ν^{-1} curves are nearly linear in this interval.[49]) To avoid interpolation error, we recorded several R'_I values very close to either side of the desired value and averaged them before interpolation. For example, to determine $\nu_{0.5}$, the voltage sweep rate where R'_I is equal to 0.50, we selected ν values to give R'_I of ~0.51−0.52 and ~0.48−0.49. Three or more determinations were made in these ranges and the average values were* then used in the interpolation. The minimum number of experimental cyclic voltammograms processed to give a single R'_I value was 18; most R'_I values were derived from >30 experimental voltammograms. The resulting ν values, for example,

(34) Grellman, K.-H.; Weller, H.; Tauer, E. *Chem. Phys. Lett.* **1983**, *95*, 195.
(35) Grellman, K.-H.; Schmitt, U.; Weller, H. *Chem. Phys. Lett.* **1982**, *88*, 40.
(36) Limbach, H.-H.; Henning, J.; Gerritzen, D.; Rumpel, H. *Faraday Discuss. Chem. Soc.* **1982**, *74*, 229.
(37) Miyazaki, T.; Shiba, T.; Fueki, K.; Kamiya, Y. *J. Phys. Chem.* **1991**, *95*, 9115.
(38) Swinney, T. C.; Kelley, D. F. *J. Phys. Chem.* **1991**, *95*, 2430.
(39) Cha, Y.; Murray, C. J.; Klinman, J. P. *Science* **1989**, *243*, 1325.
(40) Glickman, M. H.; Wiseman, J.; Klinman, J. P. *J. Am. Chem. Soc.* **1994**, *116*, 793.
(41) Hwang, C. C.; Grissom, C. B. *J. Am. Chem. Soc.* **1994**, *116*, 795.
(42) Jonsson, T.; Glickman, M. H.; Sun, S.; Klinman, J. P. *J. Am. Chem. Soc.* **1996**, *118*, 10319.
(43) Caldin, E. F.; Warrick, P.; Mateo, S. *J. Am. Chem. Soc.* **1981**, *103*, 202 and earlier work cited therein.
(44) Rogne, O. *Acta Chem. Scand.* **1978**, *A-32*, 559. Kresge, A. J.; Powell, M. F. *J. Phys. Org. Chem.* **1990**, *3*, 55.
(45) Fieser, L. F.; Heymann, H. *J. Am. Chem. Soc.* **1942**, *64*, 372.
(46) Lasson, E.; Parker, V. D. *Anal. Chem.* **1990**, *62*, 412.
(47) Moe, N. S. *Anal. Chem.* **1974**, *46*, 968.
(48) Lines, R.; Parker, V. D. *Acta Chem. Scand.* **1977**, *B31*, 369.
(49) Ahlberg, E.; Parker, V. D. *J. Electroanal. Chem.* **1981**, *121*, 73.

$\nu_{0.85}$ or $\nu_{0.5}$, were directly proportional to apparent rate constants at the extent of reaction corresponding to R'_I, that is, $R'_I = 0.85$ or 0.50 in the examples given.[50]

Digital Simulation. Digisim 2.1 (DIGI; BioAnalytical Systems, Inc., W. Lafayette, IN)[18] has 3 variable model parameters affect the accuracy of the simulation: (i) the potential step width, (ii) the exponential grid factor, and (iii) the number of iterations. The 3 parameters were varied sequentially over a factor of at least 10 while holding all other variables constant. No changes in R'_I were observed over the entire range of model parameters. The cyclic voltammograms (potential step width, 1 mV) obtained with DIGI were differentiated by the method of Savitzky and Golay.[51]

Although DIGI is the state-of-the-art software for carrying out simulation of cyclic voltammetry, we found it prohibitively time-consuming for carring out the massive number of simulations necessary to find the optimum fit between experimental and theoretical DCV data (see Results). Consequently, we developed our own simulation program to automate theoretical data collection. The simulation program is based on Feldberg's explicit finite difference (FD) method.[52] The input for the program includes experimental values of $k_{app}{}^H$, $k_{app}{}^D$, initial experimental voltage sweep rates, any number of k_f (typically 10) and any number of $k_p{}^H$ (typically 25) values at each k_f. Changes in simulation $k_p{}^H$ were accompanied by changes in k_b and $k_p{}^D$ to maintain consistency with eqs 8−10. The program simulates cyclic voltammograms for the reactions of both HA and DA, differentiates the resulting current−potential curves, assigns sweep rates necessary for each R'_I beginning at 0.85 and ending at 0.50, stores these data in files for reactions of both HA and DA, and calculates and stores KIE_{app} at each value for R'_I. All of the theoretical data for the first iteration of the data-fitting procedure can be obtained from a single input session. Each simulation requires from <1 to ~20 s, depending on the simulation potential step width, on a 350 MHz personal computer.

We used DIGI to test the reliability of the (FD) simulations. We compared the FD and DIGI simulations in the voltage sweep rate ranges where the experimental data were obtained for each of the radical cation proton-transfer reactions. Each pair of simulations gave R'_I results within 0.001 of each other (the experimental error in R'_I is around ±0.004). The comparisons are summarized in Table S1 in the Supporting Information.

Acknowledgment. We acknowledge the donors of the Petroleum Research Fund, administered by the ACS, as well as National Science Foundation (CHE-970835) for support of this research.

Supporting Information Available: Table of comparison of finite difference to digisim simulations and figures of fitting procedures (5 pages). See any current masthead page for ordering and Internet access instructions.

JA982682K

(50) Parker, V. D. *Acta Chem. Scand.* **1981**, *B35*, 233.
(51) Savitzky, A.; Golay, M. *Anal. Chem.* **1964**, *36*, 1627.
(52) Feldberg, S. W. *Electroanal. Chem.* **1969**, *3*, 199.